Environ. Sci. Technol. **2005**, *39,* 1263−1268

Quantification of the Oxidizing Capacity of Nanoparticulate Zero-Valent Iron

SUNG HEE JOO,[†] ANDREW J. FEITZ,[†]
DAVID L. SEDLAK,[‡] AND
T. DAVID WAITE*,[†]

School of Civil and Environmental Engineering,
The University of New South Wales,
Sydney, New South Wales 2052, Australia, and
Department of Civil and Environmental Engineering,
University of California, Berkeley, California 94720

Addition of nanoparticulate zero-valent iron (nZVI) to oxygen-containing water results in oxidation of organic compounds. To assess the potential application of nZVI for oxidative transformation of organic contaminants, the conversion of benzoic acid (BA) to *p*-hydroxybenzoic acid (p-HBA) was used as a probe reaction. When nZVI was added to BA-containing water, an initial pulse of p-HBA was detected during the first 30 min, followed by the slow generation of additional p-HBA over periods of at least 24 h. The yield of p-HBA increased with increasing BA concentration, presumably due to the increasing ability of BA to compete with alternate oxidant sinks, such as ferrous iron. At pH 3, maximum yields of p-HBA during the initial phase of the reaction of up to 25% were observed. The initial rate of nZVI-mediated oxidation of BA exhibited a marked reduction at pH values above 3. Despite the decrease in oxidant production rate, p-HBA was observed during the initial reaction phase at pH values up to 8. Competition experiments with probe compounds expected to exhibit different affinities for the nZVI surface (phenol, aniline, *o*-hydroxybenzoic acid, and synthetic humic acids) indicated relative rates of reaction that were similar to those observed in competition experiments in which hydroxyl radicals were generated in solution. Examination of the oxidizing capacity of a range of Fe^0 particles reveals a capacity in all cases to induce oxidative transformation of benzoic acid, but the high surface areas that can be achieved with nanosized particles renders such particles particularly effective oxidants.

Introduction

Zero-valent iron (Fe^0(s) or ZVI) has been used to remediate a variety of contaminants. In particular, reductive reactions of ZVI have been employed in permeable reactive barriers to remediate groundwater contaminated with halogenated solvents and reducible inorganic contaminants (*1*−*4*). Nanoscale zero-valent iron (nZVI) has been suggested an alternative means of exploiting the reactivity of ZVI without the need to construct passive barriers. The main advantages of nZVI are its high reactivity and the potential for introducing the particles directly into contaminated soil and groundwater (*5*, *6*).

Recently, it has been demonstrated that ZVI oxidizes organic compounds when it is used in the presence of oxygen (*7*, *8*). The byproducts observed during ZVI-mediated oxidative degradation of molinate (*7*) and phenol (*8*) are consistent with the action of a nonspecific oxidant such as the hydroxyl radical ($OH^\bullet$). The reactions that result in oxidant production are initiated when Fe^0 is oxidized by oxygen, which likely forms a reactive oxygen species either on the particle surface or in solution. The oxidation of Fe^0 by oxygen also results in the formation of a layer with properties similar to γ-Fe_2O_3 and Fe_3O_4 on the particle surface, which eventually leads to a reduction in the reactivity (or "passivation") of the surface accompanied by a decrease in the rate of Fe^0 oxidation (*9*). Formation of a surface coating of iron oxides also appears to be responsible for the decreased rate of Fe^0-mediated oxidation of organic compounds that is observed over extended time (*7*, *8*). For a system involving granular Fe^0(s), the diminution of reactivity can be counteracted by addition of a chelating agent (such as EDTA) that keeps the oxidized iron in solution (*8*). However, addition of chelating agents limits the utility of the technique for in situ treatment. The high surface area of nZVI may allow for more efficient generation of oxidants, but as reported in our previous study (*7*), a decrease in reactivity associated with the build-up of iron oxides on the surface eventually slows the reaction. If the nZVI particles continue to produce oxidants after a surface coating forms, the continued slow release of oxidants may result in degradation of contaminants present in soil and contaminated aquifers. The high surface area of the nZVI particles also could provide a means for selective oxidation of surface-active compounds.

To assess the potential applicability of nZVI for the oxidative treatment of organic contaminants, experiments were performed using the oxidation of benzoic acid (BA) to *p*-hydroxybenzoic acid (p-HBA) as a probe reaction for oxidant production. This reaction is particularly convenient as p-HBA does not adsorb strongly to either Fe^0 or iron oxide products under the conditions of interest, and the further oxidation of p-HBA by hydroxyl radicals is slow at the low concentrations of p-HBA expected to be present. Analysis of this oxidation reaction under well-defined conditions provides insight into the effect of environmental conditions (e.g., pH) on oxidation rates, the selectivity of the oxidant, and the overall efficiency of the process. Additionally, insights gained from the laboratory investigations under controlled conditions are used to assess the potential applications of this technology and to identify areas for further research.

Materials and Methods

All chemicals were high purity and were used as received. Reagents were prepared using 18 MΩ Milli-Q water. The reactions of nZVI were studied in pH-buffered solutions with an ionic strength adjusted to 0.03 M with NaCl. Benzoic acid served as the buffer at pH 3 and pH 5 while 2 mM bicarbonate was used to buffer solutions at pH 8. When necessary, the pH of the solutions was adjusted using 0.1 N HCl or 1 N NaOH. BA, p-HBA, and phenol were obtained from Sigma-Aldrich; aniline was obtained from Ajax FineChem Ltd; and humic acid was obtained from Aldrich. nZVI was synthesized as described previously (*7*). To compare the reactivity of the nZVI used in this study with other forms of Fe^0(s), studies were also undertaken with Master Builders granular ZVI (Orica Chemicals, Australia), electrolytic ZVI powder (Kanto Chemical Co., Inc, Japan), and Aldrich fine ZVI powder. The

---

* Corresponding author phone: +61-2-9385 5060; fax: +61-2-9385 6139; e-mail: d.waite@unsw.edu.au.

[†] The University of New South Wales.

[‡] University of California.

10.1021/es048983d CCC: $30.25

TABLE 1. Characteristics of ZVI Particles Used in This Study and Surface Area Normalized Generation of p-HBA by the Different Particle Types

zero-valent iron	measd BET surface area (m^2/g)[a]	literature surface area (ref) (m^2/g)	particle size (μm)	surface area normalized [p-HBA] ($\mu M/m^2$)[b]
Master Builders	0.71	1.3 ± 0.7 (*10*)	750−1200	12.0
Aldrich	0.38	0.9 ± 1.1 (*10*)	4.5−5.5	362
Kanto	0.60		100−150	149
nZVI[c]	32	31.4 (*11*)	0.001−0.2	13.6

[a] BET analyses performed on ZVI as received. [b] [p-HBA] for 1.8 mM ZVI after 1 h. [c] nZVI prepared by $NaBH_4$ reduction of $FeCl_3$ in this study.

surface area and size characteristics of these particles are given in Table 1.

p-HBA concentrations were determined by high-performance liquid chromatography (HPLC) using a Hewlett-Packard 1100 series HPLC system equipped with a 250 × 4.6 mm Waters Spherisorb ODS-2 5μ column (Alltech, IL). A two-solvent gradient elution, consisting of water (pH 3) and acetonitrile (85:15, v/v %) at a flow rate of 1.0 mL/min was used to separate BA and isomers of hydroxybenzoic acid. The p-HBA isomer was quantified at 255 nm, and BA was quantified at 270 nm. All standard curves were linear with regression coefficients of >0.9990 in all cases. The method detection limit for BA and p-HBA were 2.5 and 0.1 μM, respectively. All experiments were carried out at room temperature (20 ± 2 °C) in 100 mL serum bottles using a total volume of 50 mL. The nZVI particles were kept in suspension by placing the bottles on an orbital shaker table at 175 rotations per minute. To ensure gas exchange, the serum bottles were open to the atmosphere. Throughout the reaction, the solution pH was continuously monitored with a pH electrode. Addition of nZVI usually resulted in an initial pH increase. To maintain a constant pH, small quantities of HCl were added as needed during the first hour of the experiments. After the first hour, the pH remained constant. The pH of the suspensions was maintained within ±0.2 units of the initial values during the entire experiment.

To initiate a reaction, nZVI was added from a stock suspension to buffered solutions containing benzoic acid. Samples were collected at different time intervals in a 5 mL glass syringe. Samples were filtered immediately through a 0.45 μm Millipore (Millex AP 20) glass syringe filter. Losses of p-HBA on the filter were less than 5%, as determined by comparison of filtered and unfiltered samples collected prior to addition of nZVI. p-HBA was analyzed within 24 h of sample collection. The rates of reaction of the nZVI-generated oxidant with a range of probe compounds (aniline, phenol, *o*-hydroxybenzoic acid, and humic acid) were determined by examining the rate of production of p-HBA resulting from BA oxidation in the presence of one of the competing compounds. Experiments were also performed to assess the relative rates of hydroxyl radical oxidation of these probe compounds under conditions identical to those used in the nZVI experiments. These experiments were performed using Fenton's reagent as a source of hydroxyl radicals. Experiments were conducted in serum bottles by adding an excess (200 μM) of Fe(II) to H_2O_2 (20 μM) in pH 3, 0.03 M ionic strength solutions containing 10 mM BA. After 10 min, when less than 0.02% of the initial H_2O_2 remained, samples were collected and analyzed for p-HBA by HPLC.

Total ferrous iron was quantified by monitoring the absorbance of an Fe(II)−bipyridine complex at 522 nm. The procedure used was a variant of that described by Voelker (*12*) and consisted of premixing 0.8 mL of pH 6, 0.5 M phosphate buffer and 0.2 mL of 0.01 M bipyridine solution and adding 4 mL of unfiltered samples, followed by 0.04 mL of 0.1M Na_2EDTA. After 60 s, the samples taken from the solution at certain time intervals were filtered through a 0.22 μm Millex-GS syringe filter, and absorbance was measured at 522 nm.

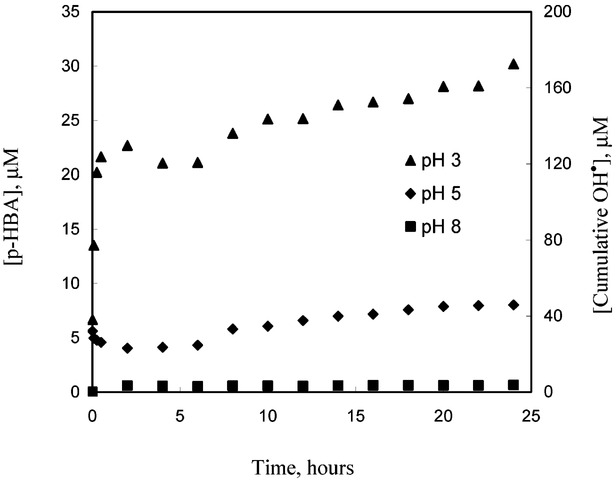

FIGURE 1. Cumulative hydroxyl radical formation and *p*-hydroxybenzoic acid concentration over time at pH 3, 5, and 8. (Conditions: 0.9 mM Fe^0, 30 mM ionic strength, and 10 mM BA.)

Results

Production of p-HBA from BA exhibited biphasic kinetics, with rapid initial production of p-HBA followed by a slow increase (apart from some variability at early times) over periods of at least 1 day (Figure 1). The concentration of p-HBA produced after 1 h was used in all subsequent experiments to compare the rates of oxidation under different conditions. Under the conditions used in these experiments (i.e., 10 mM BA; 0.9 mM nZVI), less than 5% of the BA initially present was transformed; therefore, it served as the main sink for oxidants with the result that oxidation of p-HBA was negligible. Thus, the concentration of p-HBA formed is related to the concentration of oxidizing species that could be used to transform a contaminant.

BA was transformed into three isomers of hydroxybenzoic acid. Although it was not possible to quantify each of the isomers due to difficulty resolving the ortho and meta forms, the three isomers appeared to be present at similar concentrations. The three isomers of hydroxybenzoic acid account for 90 ± 5% of the products of $OH^•$ reactions with BA with the ratio of o-HBA, m-HBA, and p-HBA products reported to be in the proportion 1.7:2.3:1.2 (*13*). For the oxidation of BA by solution-phase $OH^•$, the concentration of p-HBA has been used to estimate cumulative $OH^•$ production using eq 1 (*14*, *15*):

$$\text{cumulative OH}^\bullet\text{ produced} = [\text{p-HBA}] \times 5.87 \qquad (1)$$

A similar approach is adopted here with results from all nZVI experiments expressed in terms of both p-HBA concentration and cumulative $OH^•$ production, with the latter quantity estimated using eq 1.

To assess competition for oxidants between BA and other oxidant scavengers, such as Fe(II), experiments were conducted at pH 3 over a range of BA concentrations. The yield of p-HBA increased as BA concentrations increased from 50 μM to 5 mM and then remained approximately constant up to 20 mM (Figure 2). Simultaneous measurements of ferrous iron indicated that total Fe(II) ranged from 190 to 200 μM in almost all cases and was relatively constant over the duration of the experiment.

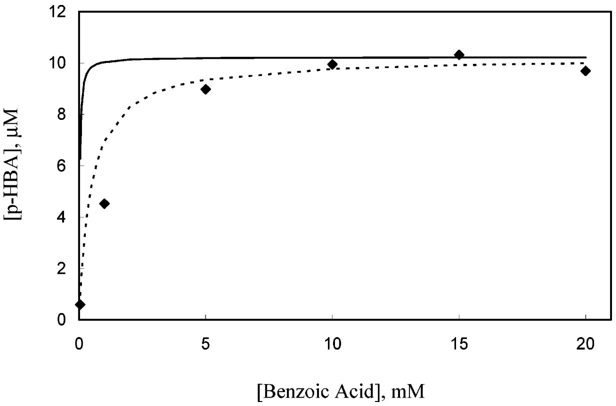

FIGURE 2. Oxidant formation as a function of benzoic acid concentration and predicted oxidant formation in the absence and presence of Fe(II) scavenging OH radicals. (Conditions: 0.9 mM Fe^0, pH 3, 30 mM ionic strength, and reaction time 1 h.) Solid and dashed lines shows calculated [p-HBA] assuming competitive hydroxyl radical scavenging by 0.2 and 5 mM Fe(II), respectively.

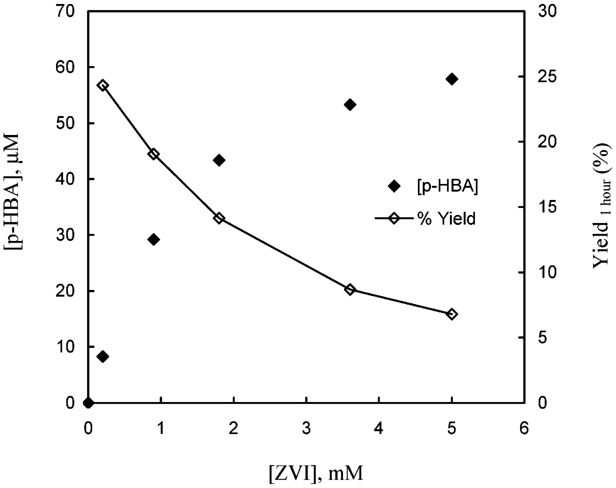

FIGURE 3. Effect of increase in nZVI concentration on concentration of p-HBA. (Conditions: 10 mM BA, 30 mM ionic strength, pH 3, and reaction time 1 h.) The yield of oxidants (i.e., [p-HBA] × 5.87) per mol of nZVI added is also shown.

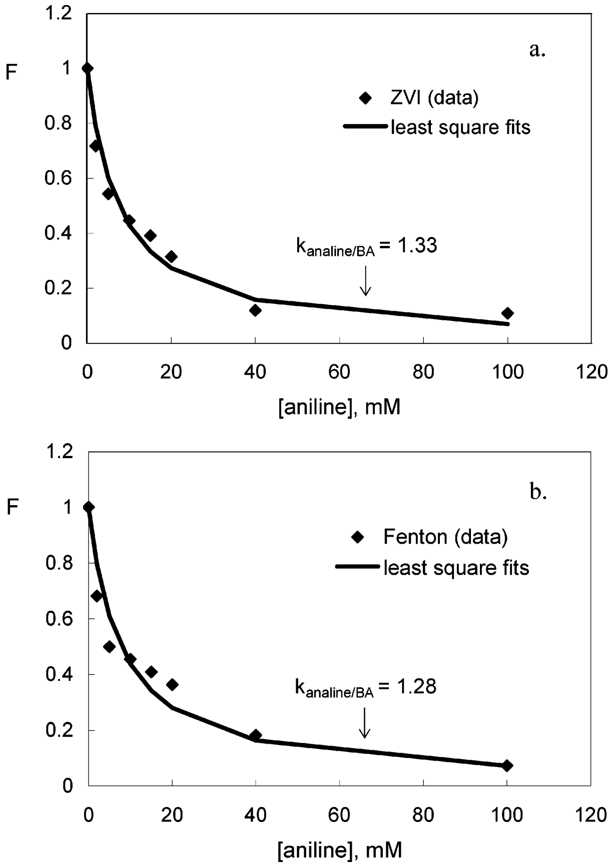

FIGURE 4. Fraction (F) of p-HBA produced in the presence of a certain concentration of aniline to that produced in the absence of aniline (i.e., in the presence of BA only) with (a) nZVI used as the oxidant source and (b) Fenton reagent used as the oxidant source.

TABLE 2. Rate Constants for Reaction of Probe Molecules with Hydroxyl Radicals Generated at pH 3 Using both nZVI and Fenton Reagant Relative to That of Benzoic Acid ($k_{C/BA}$)[a]

compound	pK_a	relative rate constant ($k_{C/BA}$) nZVI	relative rate constant ($k_{C/BA}$) Fenton	reported rate constant for reaction with OH• (k_C) ($M^{-1}s^{-1}$) (ref)
BA	4.2	1.00	1.00	4.3×10^9 (k_{BA}; *16*)
analine	4.6	1.33	1.28	$8.6 \times 10^9 - 1.7 \times 10^{10}$ (*17*)
phenol	10.0	4.65	2.28	$6.6 \times 10^9 - 1.8 \times 10^{10}$ (*17*)
o-HBA	3.0	2.62	0.32	$1.1 \times 10^{10} - 1.8 \times 10^{10}$ (*17, 18*)
humic acid	>3.6	2.74[b]	9.02[c]	

[a] Literature values for reaction of benzoic acid and probe compounds (C) with hydroxyl radicals are also shown. [b] Units of $L{\cdot}M{\cdot}s^2{\cdot}mg^{-1}$. [c] Units of L·mg·s.

Experiments conducted at pH 3 and 10 mM BA with nZVI concentrations ranging from 0.2 to 5 mM indicated an increase in pHBA production as nZVI increased (Figure 3). Assuming the same distribution of HBA isomers in the nZVI system as those observed in experiments with homogeneous OH•, these results can be used to estimate the efficiency of the initial fast reaction (i.e., the yield of oxidants per mole of nZVI added). The reaction efficiency ranged from approximately 5 to 25% with higher values at the lowest ZVI concentration.

To elucidate the selectivity of the oxidant, competition experiments were conducted with aniline, *o*-hydroxybenzoic acid, phenol, and humic acid at pH 3 and 10 mM BA. In all cases, the yield of p-HBA decreased as the concentration of the competitor increased (see Figure 4a for a typical result). The relative rate constant (i.e., the rate constant for each probe compound relative to the rate constant for BA) was estimated by a least-squares fit of the data to eq 2:

$$F = \frac{k_{BA}[BA]}{k_{BA}[BA] + k_C[C]} = \frac{1}{1 + \frac{k_C}{k_{BA}}\frac{[C]}{[BA]}} = \frac{1}{1 + k_{C/BA}\frac{[C]}{[BA]}} \qquad (2)$$

where *F* is the fraction of the p-HBA produced in the presence of a certain concentration of the competitor (C) to that in the absence of C, and $k_{C/BA}$ is the relative rate constant. Relative rate constants were also determined for the compounds in a similar manner but using Fenton's Reagent as a source of OH• (Figure 4b). Experimentally determined relative rate constants for the four probe compounds are given in Table 2 as are literature values for the absolute rate constants for reaction of the probe compounds with hydroxyl radicals.

The relative rate constants for aniline, a positively charged molecule at pH 3, are similar in both the nZVI and Fenton systems suggesting no effect of the nZVI surface on reaction rate. For phenol, the relative rate constant obtained with nZVI is twice as high as that obtained with hydroxyl radicals generated in the solution phase while the relative rate constant for humic acid with nZVI-mediated oxidation is about one-third of that found with Fenton reagent. One

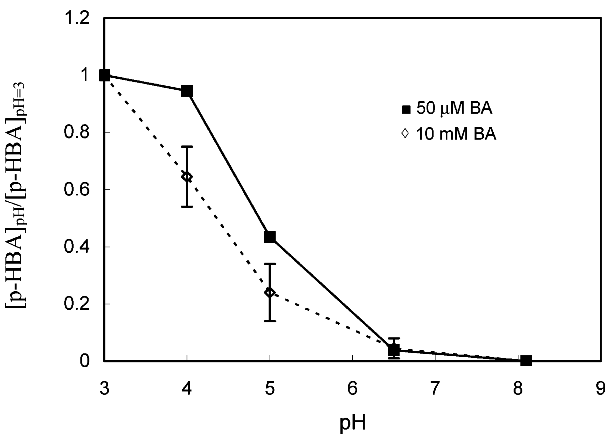

FIGURE 5. pH dependence of the formation of p-HBA. (Conditions: pH 3, 0.9 mM ZVI, ionic strength 30 mM, 50 μM and 10 mM BA, and reaction time 1 h.)

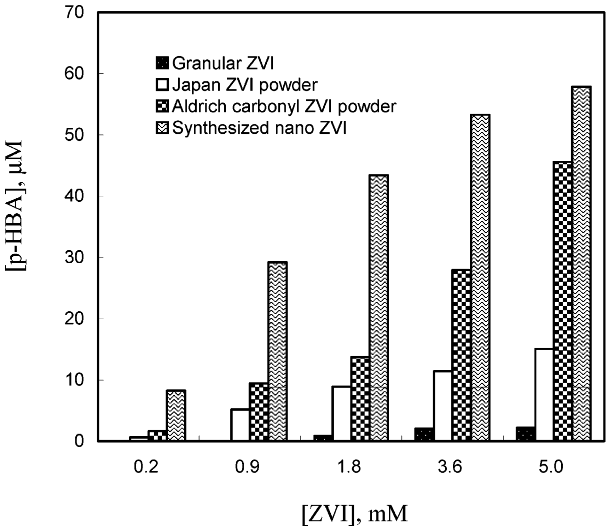

FIGURE 6. Concentration of p-HBA produced after 1 h reaction of commercial granular Fe, ZVI powders, and synthesized nZVI with benzoic acid. (Conditions: pH 3, 0.9 mM Fe^0, ionic strength 30 mM, 10 mM BA, and reaction time 1 h.)

possible explanation for the latter result is that the humic acid contains a component of relatively refractory, hydrophobic material that coats the ZVI particles lowering their reactivity. Comparison of this result with that obtained using a purified lower molecular weight fulvic acid would be of interest. Some uncertainty surrounds the quality of the relative rate data for o-HBA since the BA/o-HBA solution turned purple on adding Fe(II), presumably because of complexation between BA or o-HBA and Fe(II). Consistent with the low relative rate constant obtained in the Fenton case, this complexation might be expected to retard the rate of reaction of Fe(II) with H_2O_2 and therefore prevent the generation of $OH^{\bullet}$.

The oxidizing ability of nZVI (as measured by the extent of p-HBA production up to 1 h) as a function of pH and relative to oxidizing ability at pH 3 in the presence of 50 μM and 10 mM BA is shown in Figure 5. Despite the decrease in oxidant production rate as pH increased, oxidation was observed at pH values up to 8.

The effect of the type of ZVI was evaluated at pH 3 with 10 mM BA. All four types of ZVI particles were capable of oxidizing BA and p-HBA production increased as the total ZVI concentration increased (Figure 6). While the nZVI produced more p-HBA then the other forms of Fe^0, the rates of production for the other forms of Fe^0 were very significant. Indeed, when normalized to the measured surface area of each particle type, the Aldrich particles were found to be particularly effective in oxidizing BA (Table 1).

Discussion

The first step in the oxidation of BA by nZVI involves the oxidation of Fe^0 by O_2. One interpretation of corrosion posits the initial oxidation of Fe^0 as a 2-electron process (*19–21*):

$$Fe^0 + O_2 + 2H^+ \rightarrow Fe^{2+} + H_2O_2 \qquad (3)$$

H_2O_2 produced in eq 3 could oxidize another Fe^0:

$$Fe^0 + H_2O_2 \rightarrow Fe^{2+} + 2\ OH^- \qquad (4)$$

This process results in a 4-electron transfer and an overall stoichiometry of 2 mol of Fe^0 oxidized/mol of O_2. Alternatively, H_2O_2 could react with species such as Fe(II):

$$Fe(II) + H_2O_2 \rightarrow Fe^{3+} + OH^{\bullet} + OH^- \qquad (5)$$

These reactions could occur on the Fe^0 surface or could involve transfer of electrons through an iron oxide layer (*19*), depending upon the reaction rates and affinity of the species for surfaces. Although the 4-electron transfer process is usually the dominant mechanism of O_2-mediated corrosion, the 2-electron-transfer process can result in production of significant amounts of O_2^{2-} or H_2O_2, especially after an oxide coating has been formed on the surface. For example, in studies conducted on stainless steel rotating disk electrodes, 10–20% of the oxygen reduced during corrosion was converted into O_2^{2-} or H_2O_2 (*21*).

On Fe^0 surfaces, the initial rate of the reaction is fast. However, a surface oxide layer consisting of γ-Fe_2O_3 and Fe_3O_4-like oxides forms as the surface is oxidized (*9*). This passive layer protects the remaining Fe^0 from attack by oxygen by serving as a barrier between the Fe^0 and O_2. The initial pulse of oxidants produced in the nZVI system is consistent with oxidation of the surface Fe^0 serving as the source of oxidant. For example, assuming that each Fe^0 occupies an area equal to $1.6 \times 10^{-19}\ m^2$ (i.e., assuming an atomic radius of 1.4 Å and an Fe–Fe bond distance of 2.5 Å), a monolayer would correspond to approximately 1.8% of the total ZVI. Thus, achievement of the 25% yield of oxidants (deduced from the moles of oxidant formed per mole of nZVI added) that is observed at low nZVI doses would require that a corrosion layer of about 14 molecules in thickness is involved in the oxidation process.

Reaction 5 provides a possible explanation for the observed oxidation of BA and other organic compounds that occurs when nZVI is exposed to O_2. The simplest model for this process would involve the production of $OH^{\bullet}$ in solution followed by a homogeneous reaction between BA and $OH^{\bullet}$. In this case, the rate at which BA is oxidized would depend on the relative concentrations of different $OH^{\bullet}$ sinks. Under the conditions in our system, the dominant sinks are expected to be:

$$BA + OH^{\bullet} \rightarrow \text{intermediates} \quad k = 4.3 \times 10^9\ M^{-1}\ s^{-1}\ (16) \qquad (6)$$

$$Fe^{2+} + OH^{\bullet} \rightarrow Fe^{3+} + OH^- \quad k = 4.0 \times 10^8\ M^{-1}\ s^{-1}\ (22) \qquad (7)$$

When an aromatic compound reacts with $OH^{\bullet}$, a cyclohexadienyl radical is formed that reacts with oxygen, eventually resulting in the production of hydroxylated products (*23*, *24*). At the total Fe(II) concentrations measured in the experiments described in Figure 2 (approximately 0.2 mM), benzoic acid (eq 6) should be a dominant sink for $OH^{\bullet}$ if the reaction occurs in the bulk solution. As indicated by the calculated fit depicted in Figure 2, $OH^{\bullet}$ is scavenged more effectively than predicted by only Fe(II). Under the conditions used in these experiments, the pseudo-first-order rate constant for other unknown sinks would have to be equal to 2×10^6 s^{-1} (dashed line in Figure 2). If the sink is dissolved Fe(II), this would correspond to 5 mM Fe^{2+}.

An alternative explanation for the results depicted in Figure 2 is that hydroxyl radical is generated on or adjacent to the surface. Under such conditions, Fe(II) adsorbed on the nZVI surface or concentrated in the area immediately adjacent to the surface could more effectively compete with BA for $OH^{\bullet}$. If this were the case, we would expect organic compounds with a higher tendency to adsorb to the surface to be oxidized more quickly than those compounds with a low affinity for surfaces. At pH 3, the surface of the nZVI is positively charged (*7*). Therefore, positively charged solutes such as aniline should have a lower affinity for the surface than neutral solutes and solutes that can form surface complexes (e.g., BA or phenol). Despite the tendency for BA to exhibit a higher surface affinity than aniline, the relative rate constant for the aniline (relative to BA) is nearly identical for the nZVI system and the Fenton's reagent system in which $OH^{\bullet}$ is generated in solution (Figure 4; Table 2). The relative rates for the other solutes also do not exhibit strong selectivity for species that are expected to have a higher affinity for the surfaces.

The importance of the presence of oxygen to the ZVI-mediated oxidation process should be emphasized. It should also be noted that dissolved oxygen is likely to be initially depleted, particularly at higher ZVI concentrations. Indeed, the rate of production of oxidants (such as hydroxyl radicals) may, in some instances, be limited by oxygen depletion and the subsequent relatively slow diffusion of oxygen from the atmosphere. Some of the variability in rate of oxidant production observed in the first few hours (Figure 1) could be related to the inhomogeneity of oxygen flux to the surface following initial depletion though other factors such as transient pH changes resulting from the initial corrosion process could account for the observed changes in oxidant generation.

The apparent low selectivity observed for nZVI contrasts with the high selectivity observed in TiO_2 photocatalysis, in which the oxidant is produced at the surface. For example, the trichloroacetate anion is preferentially degraded at low pH when the TiO_2 surface ($pH_{zpc} = 6.25$) is positively charged whereas the positively charged cation chloroethylammonium is degraded preferentially at high pH when the TiO_2 surface has a net negative charge (*25*). The absence of a relationship between the charge of the compound and relative rates of oxidation in the nZVI system suggests that a direct interaction between the surface and the solute is not important. As indicated earlier, the dependence of the yield on [BA] suggests that the oxidant is not produced in the bulk solution. Therefore, it is possible that the initial oxidation occurs close to the surface in a region in which [Fe(II)] is higher than the concentrations measured in the bulk solution. The detection of mixed Fe(II)/(III) oxides such as maghemite at the nZVI surface is consistent with oxidation of Fe^{2+} to Fe(III) in these systems.

Irrespective of the identity of the oxidant or the location in which it is generated, these results indicate that oxidation of ZVI by oxygen results in the production of an oxidant that is capable of transforming organic contaminants. The initial pulse of oxidants might be useful in remediation of contaminated soils and groundwater and might serve as an alternative to other in situ treatment oxidation processes, such as the addition of H_2O_2. The slower release of oxidants that occurs after 30 min, which likely corresponds to the continued corrosion of the nZVI particle, might be useful for remediation of difficult-to-reach groundwater, provided that oxygen was not depleted from the groundwater. Additional research is needed to assess the kinetics of oxidant production from nZVI particles on the time scale of days to months.

As noted earlier and shown in Figure 3, maximum yield of oxidants per mole of nZVI added is observed at the lower doses of ZVI. The reason for the reduction in yield of oxidant on increase in ZVI concentration is unclear but may be related to the increase in concentration of ferrous iron that will accompany the increase in ZVI concentration and the increase in competitive scavenging of hydroxyl radicals that will occur as a result (eq 7). Other reasons for this reduction in yield on increase in ZVI concentration include the possibility of less efficient oxidant production as a result of oxygen diffusion limitations at the higher ZVI concentrations; however, competitive scavenging for the oxidant would seem the most likely cause.

The effect of pH reflected in the results shown in Figures 1 and 5 is interesting and worthy of further analysis. Two key observations are worth making. First, the extent of the rapid initial generation of oxidants (within the first hour) decreases markedly with increase in pH. This phenomenon may be related both to the greater affinity of the Fe° (and iron oxyhydroxide) surface for Fe^{2+} at higher pH and to the ability of O_2 to outcompete H_2O_2 for Fe^{2+} at the higher pH with a resultant reduction in rate of generation of oxidizing radicals and greater extent of generation of a passivating layer. Second, despite the significant reduction in extent of initial oxidant production at higher pH, ongoing BA oxidation is observed albeit at a lower rate than at lower pH values. Presumably, this ongoing oxidation occurs because of ongoing corrosion of the ZVI surface despite the presence of a passivating layer and ongoing reduction of oxygen to H_2O_2. It is to be expected that any oxidation that occurs at higher pH will occur at or in very close vicinity to the Fe° surface given the time taken for reactants to diffuse through the passivating layer.

The production of oxidants during Fe^0 oxidation is not a phenomenon that is limited to nZVI particles (Figure 6). Indeed, granular particles of the type commonly used in reductive barriers are observed to have similar surface area-normalized oxidizing capacity as the nZVI particles produced here, although the very low surface area of these particles would result in very low overall rates of oxidation. Interestingly, the colloidal particles obtained from Aldrich and Kanto exhibit much higher surface area normalized oxidation capacity than the nZVI particles though, again, the nanoscale nature of the sodium borohydride-produced particles results in an overall higher oxidizing capacity than other particles examined. The reason for the dramatic differences in surface area normalized reactivity however is unclear and represents a fascinating area for further study.

Acknowledgments

We thank Dr. Y.-H. Kim, School of Civil and Environmental Engineering, Andong University, for the provision of the Kanto ZVI powder and Dr. Jason Scott of the ARC Center for Functional Nanomaterials at UNSW for the BET analyses on ZVI particles. D.L.S. acknowledges the support provided by a Fulbright Senior Scholars award.

Literature Cited

(1) Gillham R. W.; O'Hannesin S. F. Enhanced degradation of halogenated aliphatics by zero-vlanet iron. *Ground Water* **1994**, *32*, 958−967.

(2) Matheson L. J.; Tratnyek P. G. Reductive dehalogenation of chlorinated methanes by iron metal. *Environ. Sci. Technol.* **1994**, *28*, 2045−2053.

(3) Agrawal A.; Tratnyek P. G. Reduction of nitro aromatic compounds by zero-valent iron metal. *Environ. Sci. Technol.* **1996**, *30*, 153−160.

(4) Farrell J., Kason M., Melitas N.; Li T. Investigation of the long-term performance of zero-valent iron for reductive dechlorination of trichloroethylene. *Environ. Sci. Technol.* **2000**, *34*, 514–521.

(5) Lien, H.-L.; Zhang, W.-X.Transformation of chlorinated methanes by nanoscale iron particles. *J. Environ. Eng.* **1999**, *125*, 1042–1047.

(6) Elliott, D. W.; Zhang, W.-X. Field assessment of nanoscale bimetallic particles for groundwater treatment. *Environ. Sci. Technol.* **2001**, *35*, 4922–4926.

(7) Joo, S. H.; Feitz, A. J.; Waite, T. D. Oxidative degradation of the carbothioate herbicide, molinate, using nanoscale zero-valent iron. *Environ. Sci. Technol.* **2004**, *38*, 2242–2247.

(8) Noradoun, C.; Engelmann, M. D.; McLaughlin, M.; Hutcheson, R.; Breen, K.; Paszczynski, A.; Cheng, I. F. Destruction of chlorinated phenols by dioxygen activation under aqueous room temperature and pressure conditions. *Ind. Eng. Chem. Res.* **2003**, *42*, 5024–5030.

(9) Davenport, A. J.; Oblonsky, L. J.; Ryan, M. P.; Toney, M. F. The structure of the passive film that forms on iron in aqueous environments. *J. Electrochem. Soc.* **2000**, *147*, 2162–2173.

(10) Alowitz, M. J.; Scherer, M. M. Kinetics of nitrate, nitrite, and Cr(VI) reduction by iron metal. *Environ. Sci. Technol.* **2002**, *36*, 299–306.

(11) Choe, S.; Lee, S.-H.; Chang, Y.-Y.; Hwang, K.-Y.; Khim, J. Rapid reductive destruction of hazardous organic compounds by nanoscale Fe^0. *Chemosphere* **2001**, *42*, 367–372.

(12) Voelker, B. Iron redox cycling in surface waters: effects of humic substances and light. Doctoral Dissertation, ETH No. 10901, Swiss Federal Institute of Technology, Zurich, 1994.

(13) Klein, G. W.; Bhatla, K.; Madhavan, V.; Schuler, R. H. Reaction of hydroxyl radicals with benzoic acid: Isomer distribution in the radical intermediates. *J. Phys. Chem.* **1975**, *79*, 1767–1774.

(14) Mopper, K.; Zhou, X. Hydroxyl radical photoproduction in the sea and its potential impact on marine processes. *Science* **1990**, *250*, 661–664.

(15) Zhou, X.; Mopper, K. Determination of photochemically produced hydroxyl radicals in seawater and freshwater. *Mar. Chem.* **1990**, *30*, 71–88.

(16) Andreozzi, R.; Marotta, R. Removal of benzoic acid in aqueous solution by Fe(III) homogeneous photocatalysis. *Water Res.* **2004**, *38*, 1225–1236.

(17) Buxton, G. V.; Greenstock, C. L.; Helman, W. P.; Ross, A. B. Critical review of rate constants for reactions of hydrated electrons, hydrogen atoms and hydroxyl radicals in aqueous solution. *J. Phys. Chem. Ref. Data* **1988**, *17* (2), 513–886.

(18) Rivas, F. J.; Beltrán, F. J.; Frades, J.; Buxeda, P. Oxidation of *p*-hydroxybenzoic acid by Fenton's reagent. *Water Res.* **2001**, *35*, 387–396.

(19) Zecevic, S., Drazic, D. M., Gojkovic, S. Oxygen reduction on iron: Part III. An analysis of the rotating disk-ring electrode measurements in near neutral solutions. *J. Electrochem. Soc.* **1989**, *265* (1–2), 179–193.

(20) Zecevic, S., Drazic, D. M., Gojkovic, S. Oxygen reduction on iron-IV: The reduction of hydrogen peroxide as the intermediate in oxygen reduction reaction in alkaline solutions. *Electrochim. Acta* **1991**, *36* (1), 5–14.

(21) Bozec, N. L.; Compère, C.; L'Her, M.; Laouenan, A.; Costa, D.; Marcus, P. Influence of stainless steel surface treatment on the oxygen reduction reaction in seawater. *Corros. Sci.* **2001**, *43*, 765–786.

(22) Sychev, A. Y.; Isak, V. G.; Pfannmeller, U. Determination of rate constants of hydroxyl radicals with organic and inorganic substances under conditions for the catalytic decomposition of hydrogen peroxide. *Zh. Fiz. Khim.* **1979**, *53* (11), 2790–2793.

(23) Dorfman L. M.; Buhler, R. E.; Taub I. A. Pulse radiolysis studies. I.Transient spectra and reaction-rate constants in irradiated aqueous solutions of benzene. *J. Chem. Phys.* **1962**, *36* (11), 3051–3061.

(24) Eberhard, M. K.; Yoshida M. Radiation-induced hemolytic aromatic substitution. I. Hydroxylation of nitrobenzene, chlorobenzene, and toluene. *J. Phys. Chem.* **1973**, *77* (5), 589–597.

(25) Kormann, C.; Bahnemann, D. W.; Hoffmann, M. R. Photolysis of chloroform an dother organic molecules in aqueous titanium dioxide suspensions. *Environ. Sci. Technol.* **1991**, *25*, 494–500.

Received for review July 2, 2004. Revised manuscript received September 23, 2004. Accepted September 28, 2004.

ES048983D